104 (2025) 105329

Contents lists available at ScienceDirect

Poultry Science

journal homepage: www.elsevier.com/locate/psj

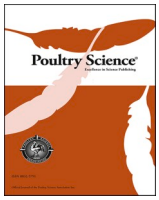

Transcriptomic analysis of the liver, jejunum, and uterus in different production stages of laying hens

Gi Ppeum Han, Byeonghwi Lim, Jun-Mo Kim, Deok Yun Kim, Hyun Woo Kim, Dong Yong Kil *

Department of Animal Science and Technology, Chung-Ang University, Anseong-si, Gyeonggi-do 17546, Republic of Korea

ARTICLE INFO

Keywords:
Gene co-expression network
Laying hen
Multi-tissue
Laying stage
Transcriptome

ABSTRACT

Egg production in laying hens is related to very complex and elaborate processes involving the cooperation of various tissues. Laying hens undergo this complicated production process in different production stages during overall laying periods. However, many previous studies have focused on a single tissue or specific production stage. Thus, we compared multi-tissue transcriptome profiles across different production stages using RNA-seq to understand which overall metabolic changes occur in laying hens as the stage progresses. Laying hens at three distinct production stages of early-phase (EP, 30 wk of age), mid-phase (MP, 46 wk of age), and late-phase (LP, 60 wk of age) were used to analyze transcriptomic changes for the liver, jejunum, and uterus tissues. Weighted gene co-expression network analysis was adopted to detect core modules and central genes, and finally identified 11 co-expression modules. In the liver and jejunum, the expression of genes (e.g., *FABP2, FABP7, PPARG*) related to fatty acid synthesis was increased with production stages. However, the expression of genes (e.g., *GSTA2, BLB1* and *BLB2*) related to immune responses, including xenobiotic metabolism pathway and the herpes simplex virus 1 infection pathway, was increased in EP compared with other stages. Moreover, the expression of genes related to calcium signaling pathways (e.g., *CACNA2D1*) and muscle contraction metabolism (e.g., *ACTG2* and *RYR2*) in the uterus was decreased as laying hens were aged. The current findings pave the way for future investigations into the physiological changes in laying hens across different production stages. This research also provides a foundation for elucidating the multi-tissue transcriptome in laying hens and identifying potential genes regulating various biological processes during overall laying periods.

Introduction

Eggs are one of the most important animal products contributing to a sustainable food supply worldwide (El-Sabrout et al., 2022). The commercial laying hen is usually raised for over a year, leading to an aging with problems in physiological functions and health (Hao et al., 2021), which impairs productive performance and egg quality (Kim et al., 2014; Chen et al., 2021; Guo et al., 2022). Many efforts have been made towards maintaining the quality and quantity of eggs that aging hens produce; yet the results have been less promising (Boling et al., 2000; Skřivan et al., 2010; de Juan et al., 2023). One reason for these unsuccessful outcomes may be due to the lack of information regarding how molecular functions in various body tissues change during aging of laying hens.

Laying hens undergo complex processes to produce a single complete egg in the oviduct from an ovulated yolk (Kaspers, 2016). In particular, the uterus is the segment where the calcified shell is formed, which is the most time-consuming process and determines overall eggshell quality (Mishra et al., 2019). The liver, as the central organ for nutrient metabolism, also plays an essential role in egg formation by participating in the synthesis of egg yolk and the transport of Ca (Galea, 2011). Depending on the nutrient requirement of laying hens, the small intestine, along with others, regulates nutrient digestion, absorption, and utilization (Omotoso et al., 2021). Furthermore, it has been appreciated that the gastrointestinal (**GIT**) function and health affect laying performance in various ways, such as intestinal barrier functions and microbial compositions (Gu et al., 2021a). Despite the significant roles of those 3 organs in egg production, their functional interrelationship at the molecular level is largely unknown. Moreover, functional changes in specific organs related to egg production may be highly dependent on aging

Scientific section: Genetics and Molecular Biology

* Corresponding author.
E-mail address: dongyong@cau.ac.kr (D.Y. Kil).

https://doi.org/10.1016/j.psj.2025.105329
Received 30 March 2025; Accepted 21 May 2025
Available online 22 May 2025

Table 1
Composition and nutrient contents of layer diets during the experiment (as-fed basis).

Item	Feeding phase (age)		
	30 – 34 wks	35 – 50 wks	51 – 60 wks
Ingredients (%)			
Corn	63.97	65.39	64.88
Soybean meal	11.24	15.93	13.03
Corn gluten meal	10.93	5.80	5.32
Wheat bran			3.00
Monodicalcium phosphate	1.85	1.48	1.32
Limestone	10.05	9.70	10.29
L-Lysine H_2SO_4	0.62	0.32	0.40
DL-Methionine	0.23	0.21	0.23
L-Threonine	0.11	0.05	0.08
L-Tryptophan	0.31	0.15	0.17
Celite		0.28	0.59
NaCl	0.30	0.30	0.30
Choline	0.05	0.05	0.05
Antioxidant	0.01	0.01	0.01
$NaHCO_3$	0.10	0.10	0.10
Vitamin premix[1]	0.10	0.10	0.10
Mineral premix[2]	0.13	0.13	0.13
Total sum	100.00	100.00	100.00
Calculated nutrient and energy content[3]			
AME_n, kcal/kg	2,860	2,800	2,770
Crude protein, %	17.05	15.92	14.79
SID Lysine, %	0.81	0.73	0.71
SID Methionine + Cysteine, %	0.69	0.63	0.62
SID Threonine, %	0.57	0.52	0.50
SID Tryptophan, %	0.18	0.17	0.16
Total calcium, %	4.08	3.91	4.09
Available phosphorus, %	0.45	0.38	0.35

[1] Provided per kg of the complete diet: vitamin A, 10,000 IU; vitamin D3, 4,500 IU; vitamin K3, 3.0 mg; vitamin B1, 2.50 mg; vitamin B2, 6.50 mg; vitamin B6, 3.20 mg; vitamin B12, 18.0 μg; biotin, 180 μg; folic acid, 1.9 mg; niacin, 60 mg.
[2] Provided per kg of the complete diet: cobalt, 1,200 μg ($CoSO_4$); copper, 19.0 mg ($CuSO_4$); iron, 72 mg ($FeSO_4$); iodine, 1.5 mg ($Ca[IO_3]_2$); manganese, 144.0 mg (MnO); selenium, 360 μg (Na_2SeO_3); zinc, 120 mg ($ZnSO_4$).
[3] Calculated values from Hy-Line Brown International (2016).

of laying hens. However, few studies have simultaneously looked at molecular functions in several pivotal tissues involved in egg production while considering different production stages of laying hens.

Transcriptome analysis is increasingly conducted in various fields of poultry science to investigate molecular and functional alterations by genotypes, aging, diets, and environment (Han et al., 2023; Kim et al., 2023; Malila et al., 2024). Therefore, the current study aimed to conduct a multi-tissue transcriptomic analysis with the liver, jejunum, and uterus to identify the role and regulation of differentially expressed genes (**DEGs**) associated with age-dependent physiological functions in laying hens.

Materials and methods

Animals and tissue collection

All experimental procedures were reviewed and approved by the Animal Care and the Use Committee at Chung-Ang University. A total of 128 30-wk-old Hy-Line Brown laying hens were allocated into 8 groups with 16 birds per group in the early-phase of production stage (**EP group**). All hens originated from the same flock and were fed a diet containing recommended levels of energy and nutrients under the same experimental conditions for 12 wks before the beginning of the current study. Hens were placed in individual cages (24 × 36 × 39 cm) in an environment-controlled room. Eight hens (one hen per group) with average body weight (**BW,** 1.86 kg) of the group were immediately chosen and euthanized to collect the liver, jejunal mucosa, and uterus tissues. Other hens were continuously raised for an additional 16 wk, and then eight hens with an average BW (1.97 kg) of the group were selected to collect 3 tissue samples (i.e., 46 wk of age at the mid-phase of production stage, **MP group**). Finally, the remaining hens were raised for additional 14 wks, and eight hens with an average BW (2.04 kg) of the group were selected to collect tissue samples again (i.e., 60 wk of age at the late-phase of production stage, **LP group**). All hens were fed 3 sequential phase diets containing recommended levels of energy and nutrients from 30 wks and 60 wks of age (Hy-Line Brown International, 2016, Table 1). All hens were raised under a programmed lighting (16L:8D) and received a periodic ventilation to maintain room temperature and humidity throughout the entire study, according to the management guideline of Hy-Line Brown International (2016).

The selected hens (i.e., 8 hens per each stage) were continuously monitored every 30 min from 4 a.m. to 2 p.m. on the day before sampling to decide the oviposition time. All hens were euthanized by CO_2 asphyxiation at 6 h after their oviposition, which is considered the initiation period of calcification in the uterus (Zhang et al., 2019). All tissue samples (i.e., liver, jejunal mucosa, and uterus) were rapidly harvested, washed with phosphate-buffered saline, immediately frozen in liquid N, and then stored at −80°C until further RNA extraction analysis. The detailed procedure of tissue sampling is presented in Fig. 1.

Total RNA extraction, cDNA library construction, and RNA-sequencing

A total of 72 tissue samples (8 liver, 8 jejunal mucosa, and 8 uterus samples from each production stage) were used to extract total RNA. The extraction was performed using TRIzol reagent (Invitrogen, Carlsbad, CA, USA) after grinding the frozen tissue samples under liquid N conditions. The RNA integrities of all 72 samples were assessed using an Agilent Technologies 2100 Bioanalyzer and RiboGreen dye (Invitrogen, Carlsbad, CA, USA), with quantification carried out using a Trinean DropSense96 spectrophotometer (Trinean, Gentbrugge, Belgium). Quality control criteria were set as a ratio of 28S:18S > 1 and RNA integrity number (**RIN**) > 7. Only high-quality RNA extracts that met these criteria were used for library preparation (Han et al., 2023).

Consequently, 33 out of the 72 RNAs, which met high-quality control criteria, were subjected to further RNA-seq analysis (i.e., 5 liver, 3 jejunal mucosa, and 3 uterus samples from each production stage). The cDNA libraries were synthesized from the total RNA using the TruSeq Stranded mRNA Sample Preparation Kit (Illumina, San Diego, CA, USA) following previously described methods (Han et al., 2021). The library fragments were purified from the total RNA with the AMPure XP bead (Beckman Coulter, Beverly, MA, USA) to obtain cDNA fragments before constructing the cDNA libraries. A total of 33 cDNA libraries were prepared for high-throughput sequencing and performed on the Illumina Nextseq 500 platform (Illumina, San Diego, CA, USA), generating paired-end reads of 2 × 75 bases.

Transcriptomic sequencing analysis

The quality of the raw reads for each sample was assessed using FastQC v0.11.7 (Andrews, 2010). The raw reads containing adapters, poly N and low-quality reads were cleaned using Trimmomatic v0.38 (Bolger et al., 2014). Processed high-quality reads were then mapped to the chicken reference genome (*GRCg6a*, GCA_000002315.5) from the Ensembl genome browser (http://www.ensembl.org/Gallus_gallus/) using HISAT2 software v2.1.0 (Kim et al., 2015). The mapped reads were sorted, and their summary was obtained at the gene level using the featureCounts v1.6.3 with Ensembl annotation v100 (Liao et al., 2014). Differential expression analysis of the genes was performed using edgeR v3.26.5 in the R. The trimmed mean of M-value (**TMM**) method was applied for normalization of the raw counts (Robinson et al., 2010; Robinson and Oshlack, 2010). All DEGs were identified by comparing with the gene expression levels at older production stages relative to those at younger production stages in laying hens (i.e., MP vs. EP, LP vs.

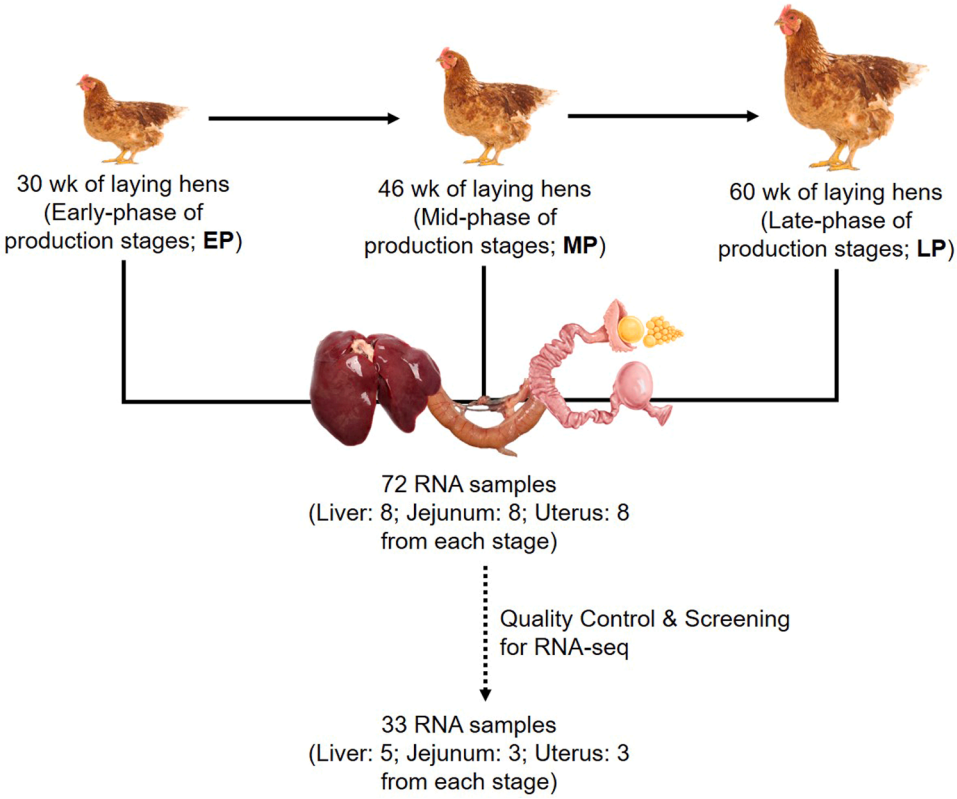

Fig. 1. The experimental design for RNA-sequencing (RNA-Seq) study. Three different productive stages (early, mid, and late-phase) were used for RNA-seq. Eight hens from each stage were selected to collect the liver, jejunal mucosa, and uterus tissues for RNA-Seq. Finally, 33 (3 different productive stages × 3 tissues; 5 liver, 3 jejunum, and 3 uterus) out of the 72 (3 different productive stages × 3 tissues; 8 liver, 8 jejunum, and 8 uterus) RNAs were subjected to RNA-seq.

MP, and LP vs. EP). The genes with a false discovery rate (**FDR**) < 0.05 and an absolute $\log_2$ fold-change (**FC**) ≥ 1 were assigned as the threshold for DEGs. The sequencing data were submitted to the NCBI Sequence Read Archive database under the accession number PRJNA1073593.

A Venn diagram illustrating the shared and unique genes among samples was created using the online website (http://jvenn.toulouse.inra.fr/app/example.html). The overall similarity between samples was conducted using a multidimensional scaling (**MDS**) with the R package "limma" (Smyth, 2005). To identify key pathways associated with the DEGs, Gene Ontology (**GO**) and Kyoto Encyclopedia of Genes and Genomes (**KEGG**) pathway enrichment analyses were conducted using the Database for Annotation, Visualization and Integrated Discovery (**DAVID**; Dennis et al., 2003). The functional gene analysis was based on the *Gallus gallus* reference. The GO enrichment analysis was performed for biological process (**BP**), cellular component (**CC**), and molecular function (**MF**). The *P*-value < 0.1 and counts ≥ 2 were used as cut-off criteria.

The weighted gene co-expression network analysis (**WGCNA**) package in R was used to construct the co-expression network for all DEGs in different tissues at different production stages (Langfelder and Horvath, 2008). Log_2-transformed TMM values for DEGs across samples were used to create background networks that reflect phenotypic characteristics (tissues and production stages) using the 'WGCNA' package v1.7.1 in R. The relationships between modules and traits were assessed using Spearman correlations for qualitative variables. Co-expression networks were visualized using Cytoscape v3.9.1, where the nodes represented DEGs and edges indicated significant interactions.

Validation of differentially expressed genes (DEG) identification by quantitative reverse transcription polymerase chain reaction (qRT-PCR)

For validation of the results obtained from RNA-seq analysis, quantitative reverse transcription polymerase chain reaction (**qRT-PCR**) was performed using the same RNA samples that were used for RNA-seq, following the previously described protocol (Han et al., 2023). The primer sequences for RT-PCR were designed using the Primer-BLAST tool in the NCBI and their details can be found in Supplementary Table S1. Briefly, cDNA was synthesized using the RevertAid First Strand cDNA Synthesis Kit (Thermo scientific, Waltham, USA) according to the manufacturer's instructions. The RT-PCR amplifications were carried out in 20 μL PCR reaction mixture containing, which included 1 μL of diluted cDNA (100 ng), 10 μL of AMPIGENE® qPCR Green Mix Lo-ROX (Enzo life science, Farmingdale, NY, USA), 1 μL of each forward and reverse primer (10 pmol), and 7 μL of nuclease-free water. The RT-PCR was performed using a CFX Connect real-time PCR Detection system (Bio-Rad, CA, USA). The cycling conditions were as follows: an initial denaturation at 95°C for 2 min, followed by 40 cycles of amplification (95°C for 5 s and the specific annealing temperature for 25 s). The relative quantification of gene expression levels was determined by normalizing to chicken glyceraldehyde-3-phosphate dehydrogenase (***GAPDH***) and using $2^{-\Delta\Delta Ct}$ method.

Results

Overview of RNA-sequencing quality assessment

A total of 685.7 million paired-end sequence reads were obtained from the 33 libraries (comprising 3 tissues and 3 production stages) with an average of 20.8 million reads in each sample (range: 17,246,755 ~ 24,450,640). The GC content of the libraries ranged from 47 to 51 %, which were very close to 50 % (Supplementary Table S2). More than 95.71 % of the reads could be mapped to the *Gallus gallus* 6.0 assembly of the chicken genome (EP: 94.59 to 96.76 %; MP: 95.40 to 97.29 %; LP: 93.85 to 95.89 % alignment), and the average unique mapping rate was 90.44 %, ranging from 88.42 to 91.89 %.

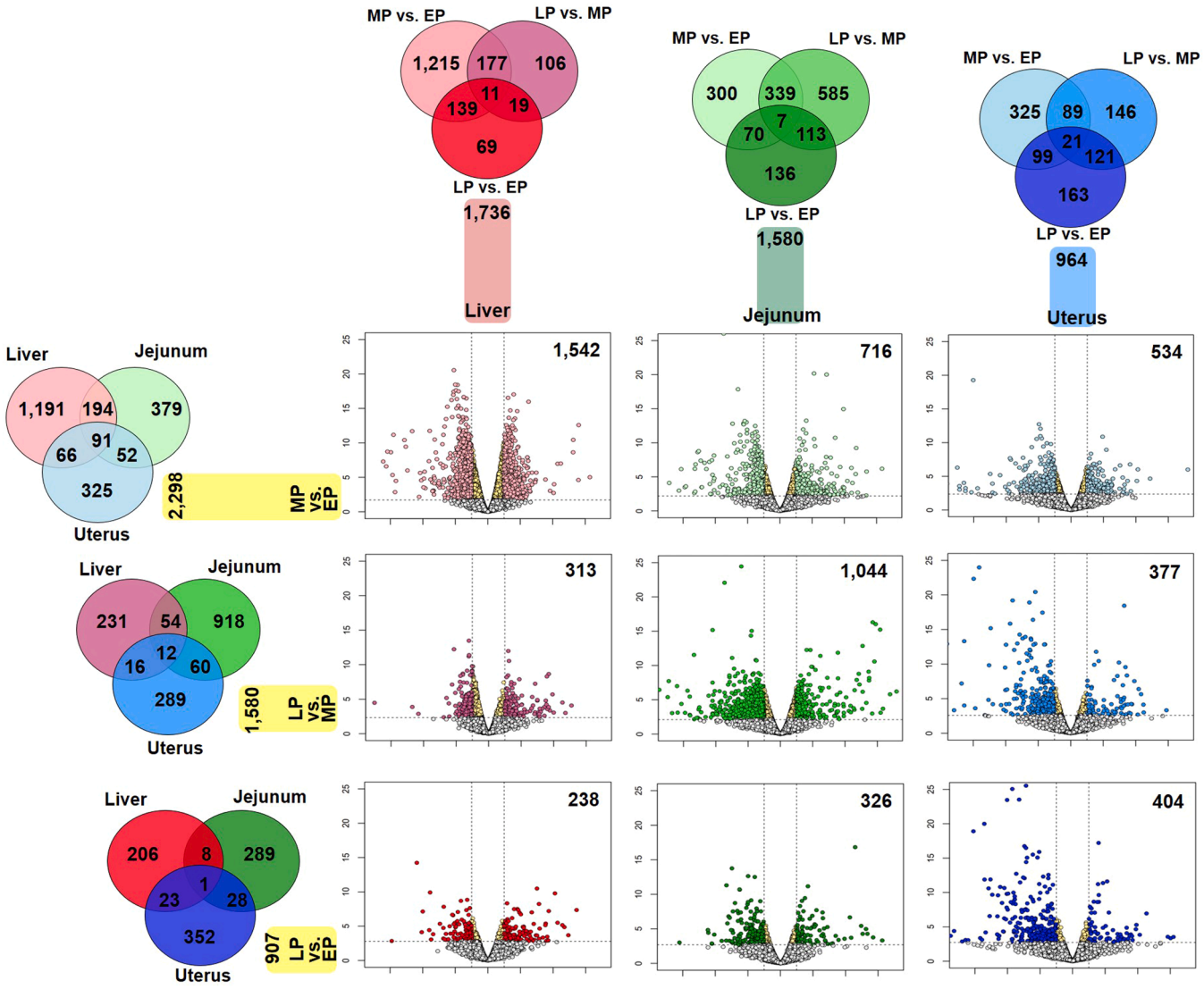

Fig. 2. Transcriptomes in different tissues and different productive stage of laying hens. Dynamic view according to productive stage in laying hens. The x and y axes of the volcano plots show the $\log_2$ FCs and $-\log_{10}$ P values, respectively. Data information: significant DEGs (FDR < 0.05 and absolute $\log_2$ FC ≥ 1) are represented in the volcano plots, with 3 different colors (red, green, and blue) corresponding to each tissue, and the numbers of DEGs are written in the top right corner of each plot. Volcano plots and Venn diagrams for different time points are indicated with color gradients. Tissue-specific Venn diagrams are illustrated with a color gradient, based on overlapping numbers of DEGs at different production stages. Venn diagrams with scale bars show the numbers of integrated DEGs observed at each stage for each tissue.

Differentially expressed genes (DEGs) profiling

In total, 16,151 genes were detected in the 33 sequencing samples of multiple tissues in laying hens at three productive stages. The details of all DEGs are presented in Supplementary Table S3. In the liver, a total of 1,736 DEGs were obtained from MP vs. EP, LP vs. MP, and LP vs. EP, of which 1,542, 313, and 238 DEGs were identified in MP vs. EP, LP vs. MP, and LP vs. EP, respectively (Fig. 2). In the jejunum, a total of 1,580 DEGs were obtained from MP vs. EP, LP vs. MP, and LP vs. EP, of which 716, 1,044, and 326 DEGs were identified in MP vs. EP, LP vs. MP, and LP vs. EP, respectively. In the uterus, a total of 964 DEGs were obtained from MP vs. EP, LP vs. MP, and LP vs. EP, of which 534, 377, and 404 DEGs were identified in MP vs. EP, LP vs. MP, and LP vs. EP, respectively.

As shown in Fig. 2, 1,542, 716, and 534 DEGs were obtained from the liver, jejunum, and uterus in MP vs. EP, respectively. The number of DEGs for the liver, jejunum, and uterus were 313, 1,044, and 377 in LP vs. MP, respectively. The number of DEGs for the liver, jejunum, and uterus were 238, 326, and 404 in LP vs. EP, respectively.

Based on the identified DEGs of the intersection of MP vs. EP, LP vs. MP, and LP vs. EP, total 11, 7, and 21 genes were commonly found in the liver, jejunum, and uterus, respectively (Table 2 and Fig. 2). Moreover, the intersection of the liver, jejunum, and uterus included 91, 12, and 1 genes in MP vs. EP, LP vs. MP, and LP vs. EP, respectively (Table 3 and Fig. 2).

The MDS plots of the DEGs were visualized for their transcriptional profiles between multiple tissues and different production stages (Fig. 3). MDS plots demonstrated that the same tissue clustered together, regardless of production stages, indicating obvious functional differences among 3 tissues in laying hens.

GO and KEGG analysis for DEGs in the intersection

Functional enrichment analysis was performed based on DEGs of the intersection in different production stages and different tissues of laying hens. However, a significant GO result was only found in the intersection of MP vs. EP of the liver, jejunum, and uterus among 6 intersection

Table 2
The intersection genes of different production stages in the liver, jejunum, and uterus of laying hens.

Category	Number of intersection genes[1]	Ensemble name	Gene name	Most up stage[2]	Most down stage[3]
Liver	11	ENSGALG00000002845	*CTNNA3*	LP	EP
		ENSGALG00000030908	*ATP2B2*	LP	EP
		ENSGALG00000000357	*ADAMDEC1*	LP	EP
		ENSGALG00000002517	*TMEM35B*	EP	MP
		ENSGALG00000011856	*FMC1*	EP	MP
		ENSGALG00000052702	uncharacterized	EP	MP
		ENSGALG00000030941	*KIAA1324*	EP	MP
		ENSGALG00000028451	*MT4*	EP	MP
		ENSGALG00000027874	*CHAC1*	EP	MP
		ENSGALG00000044735	uncharacterized	EP	MP
		ENSGALG00000024085	*IDO2*	EP	LP
Jejunum	7	ENSGALG00000016954	*RGCC*	LP	EP
		ENSGALG00000020386	*BDKRB1*	MP	LP
		ENSGALG00000038396	uncharacterized	MP	LP
		ENSGALG00000023552	*SPEF2*	EP	LP
		ENSGALG00000044661	uncharacterized	EP	LP
		ENSGALG00000049716	uncharacterized	EP	LP
		ENSGALG00000051946	uncharacterized	EP	LP
Uterus	21	ENSGALG00000016600	*POMC*	MP	LP
		ENSGALG00000054544	uncharacterized	MP	LP
		ENSGALG00000015419	*PENK*	MP	LP
		ENSGALG00000013568	*NR4A3*	MP	LP
		ENSGALG00000033695	*CYP26A1*	MP	LP
		ENSGALG00000010551	*CDC42EP3*	MP	LP
		ENSGALG00000003521	*TPM1*	EP	LP
		ENSGALG00000001918	*DNAJB5*	EP	LP
		ENSGALG00000012715	*CAP2*	EP	LP
		ENSGALG00000014995	*PGM5*	EP	LP
		ENSGALG00000007226	*OSTN*	EP	LP
		ENSGALG00000016797	*FHL2*	EP	LP
		ENSGALG00000054718	*FLNA*	EP	LP
		ENSGALG00000028721	*LMOD1*	EP	LP
		ENSGALG00000011865	*SMTN*	EP	LP
		ENSGALG00000041266	*CNN1*	EP	LP
		ENSGALG00000011306	*DES*	EP	LP
		ENSGALG00000028567	*MYL9*	EP	LP
		ENSGALG00000011902	*TAGLN*	EP	LP
		ENSGALG00000041634	*ACTG2*	EP	LP
		ENSGALG00000011086	*ACTA1*	EP	LP

Abbreviation: EP, early-phase of production stages (30 wk); MP, mid-phase of production stages (46 wk); LP, late-phase of production stages (60 wk).
[1] Number of intersection genes = the number of intersection genes in MP vs. EP, LP vs. MP, and LP vs. EP.
[2] Most up stage refers to the stage with the highest expression value among three different production stages (EP vs MP vs LP).
[3] Most down stage refers to the stage with the lowest expression value among three different production stages (EP vs MP vs LP).

Table 3
The intersection genes of the liver, jejunum, and uterus at two different production stages in laying hens.

Category	Number of intersection genes[1]	Ensemble name	Gene name	Fold change (log_2)		
				Liver	Jejunum	Uterus
MP vs. EP	91	-	-	-	-	-
LP vs. MP	12	ENSGALG00000039205	*CCT3*	2.01	1.96	2.26
		ENSGALG00000028451	*MT4*	1.89	1.47	1.11
		ENSGALG00000028145	*BORCS6*	1.57	1.98	1.01
		ENSGALG00000050002	*COLE11*	−1.07	−2.09	−2.46
		ENSGALG00000017042	*UFM11*	−1.21	−1.05	−1.11
		ENSGALG00000008486	*CACNA2D1*	−1.39	−1.43	−1.52
		ENSGALG00000012766	*SYCP3*	−1.47	−1.61	−1.67
		ENSGALG00000041500	uncharacterized	1.62	1.44	2.04
		ENSGALG00000051810	uncharacterized	1.24	1.07	1.28
		ENSGALG00000037737	uncharacterized	1.21	1.15	1.57
		ENSGALG00000053342	uncharacterized	−2.13	−2.42	−2.29
		ENSGALG00000051082	uncharacterized	−3.07	−3.46	−2.15
LP vs. EP	1	ENSGALG00000041634	*ACTG2*	−2.34	1.46	−4.93

Abbreviation: EP, early-phase of production stages (30 wk); MP, mid-phase of production stages (46 wk); LP, late-phase of production stages (60 wk).
[1] Number of intersection genes = the number of intersection genes in the liver, jejunum, and uterus of laying hens.

results (Fig. 4). The result revealed that DEGs were enriched to 21 different GO terms including 10 BP terms, 5 CC terms, and 6 terms (*P*-value < 0.1). The most significantly GO terms included mitochondrial respiratory chain complex I assembly (GO:0032981), detoxification of copper ion (GO:0010273), and cellular oxidant detoxification (GO:0098869) in BP terms.

Co-expression network analysis of DEGs in different tissues and different production stages

The WGCNA was performed to construct the co-expression network of DEGs identified in the liver, jejunum, and uterus according to different production stages in laying hens. The results indicated that

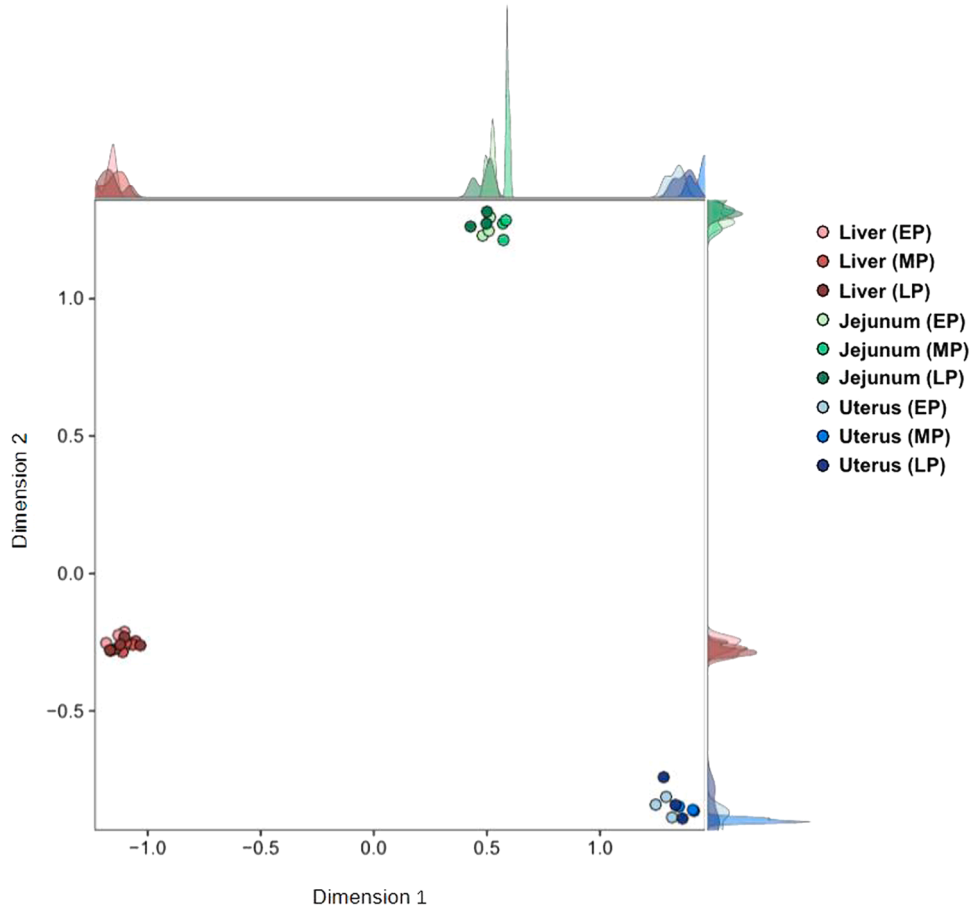

Fig. 3. The multidimensional scaling (MDS) plot showing the expression level of genes in 33 different samples (3 tissues based on the transcriptomes at 3 different production stages). Red spot represents liver tissue, green spot represents jejunum tissue, and blue spot represents uterus tissue. As age increases, there was a darker appearance noted in the color of the spots.

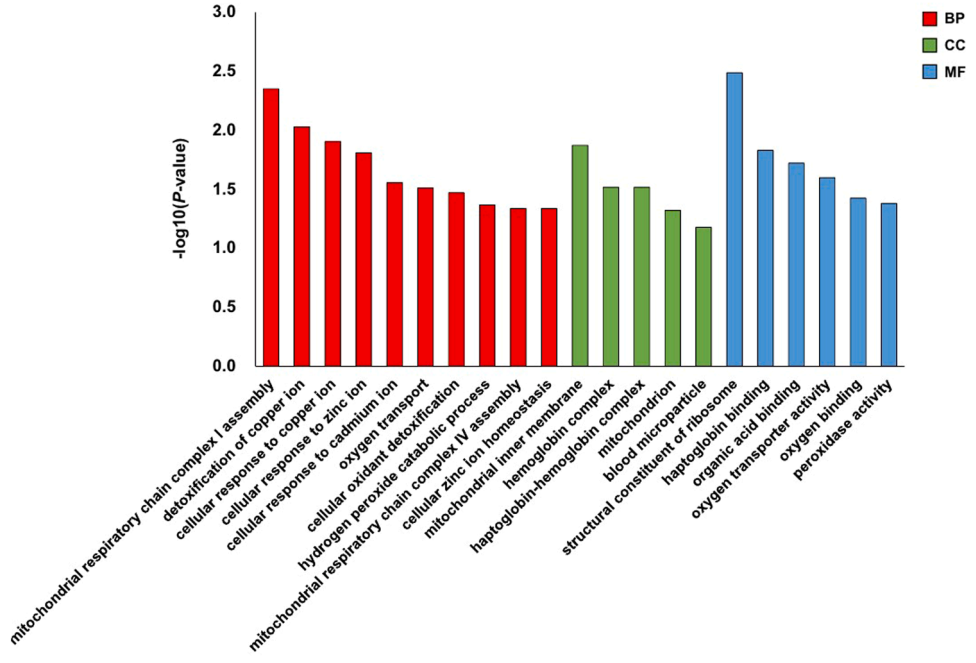

Fig. 4. Most significantly enriched gene ontology (GO) terms associated with 91 differentially expressed genes between the intersection of MP vs. EP of the liver, jejunum, and uterus in laying hens. GO categories, including biological processes (BP), cellular components (CC), and molecular functions (MF), are shown in red, green, and blue color, respectively.

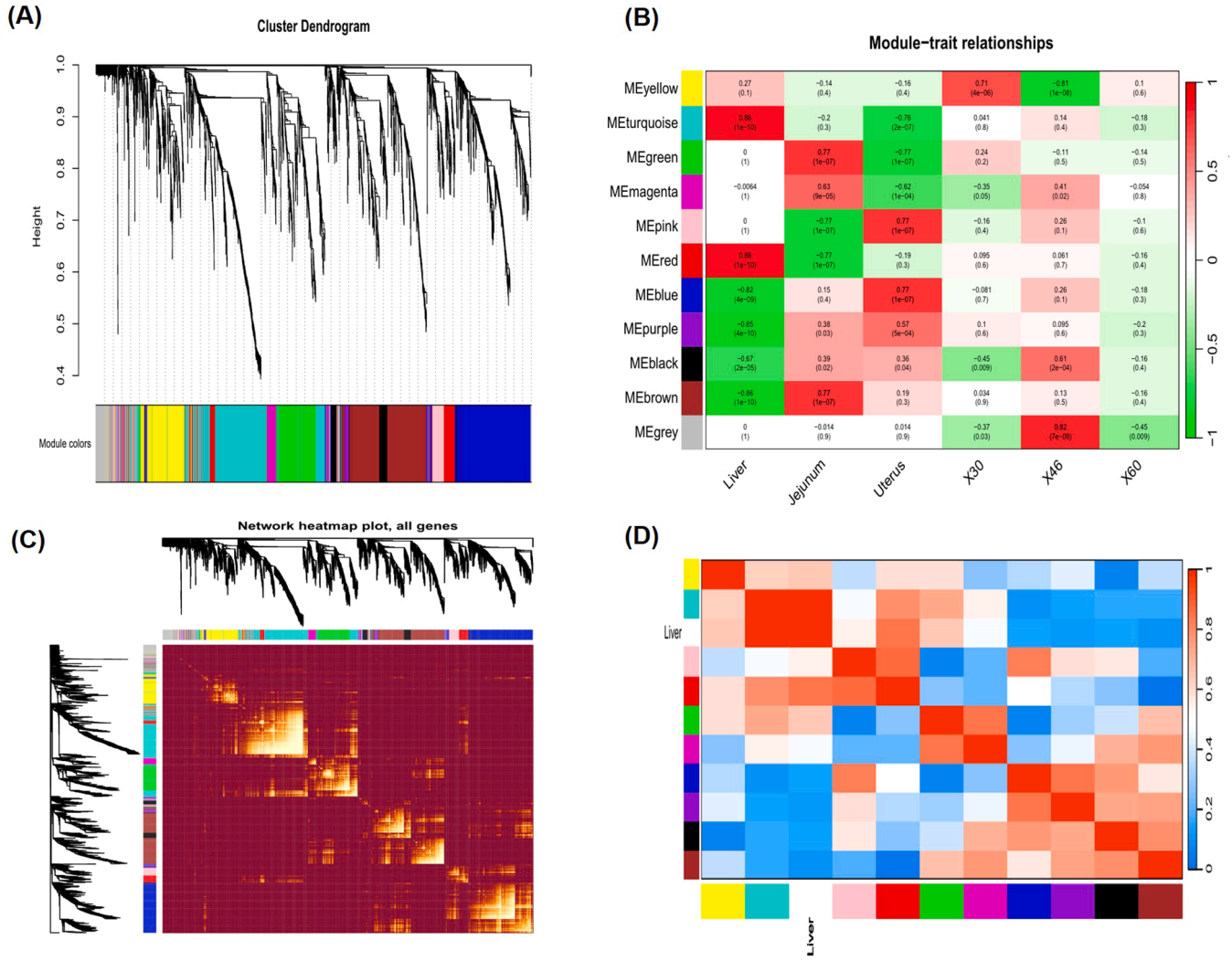

Fig. 5. The result of weighted gene co-expression network analysis. (A) Hierarchical clustering diagram. Different colors on abscissa represent different clustering modules. (B) Correlation between modules and groups. The abscissa represents tissues with different productive stage groups, and ordinate represents different module. (C) Visualized network heat map. (D) Correlation diagrams between modules. The redder the color of the area of different modules, the stronger the correlation.

genes with similar expression patterns in the liver, jejunum, and uterus were categorized with 11 modules (Fig. 5). Afterwards, correlation analysis between the phenotypes and modules demonstrated that genes clustered in the 'Turquoise' modules were intensely correlated with the liver (Figs. 5B and 6). Moreover, genes clustered in the 'Green' and 'Brown' modules were correlated with the jejunum, whereas genes clustered in the 'Blue' modules were correlated with the uterus.

Subsequently, KEGG enrichment pathway analysis revealed that 12, 11, 9, and 6 KEGG pathways were enriched in 'Turquoise', 'Green', 'Brown', and 'Blue' modules, respectively (Fig. 7). Metabolic, steroid biosynthesis, PPAR signaling pathway, xenobiotic metabolism significantly enriched by DEGs in the turquoise module (Figs. 7A, 8A, and 8B). Several metabolism-related KEGG pathways were enriched by DEGs in the green module, including herpes simplex virus 1 infection, intestinal immune network for IgA production, arginine and proline metabolism, and histidine metabolism pathways (Figs. 7B and 9). Furthermore, DEGs in the brown module were mainly enriched in calcium signaling pathway, PPAR signaling pathway, and cytokine-cytokine receptor interaction pathways (Figs. 7C and 10). Moreover, DEGs in the blue module were also enriched calcium signaling pathway, apelin signaling pathway, and mTOR signaling pathway (Figs. 7D and 11).

Validation of differentially expressed gene (DEG) in the RNA-sequencing data

To validate RNA-seq expression results, 9 DEGs, including 3 up-regulated genes (*XIRP1, VTG1*, and *APOA4*) and 6 down-regulated genes (*FABP2, ORM1, ELOVL7, IDO2, KCNK17*, and *CA4*), were randomly selected using qRT-PCR (Fig. 12). The linear regression confirmed a strong relationship between RNA-seq and qRT-PCR data, which validated the current RNA-seq results.

Discussion

The largest number of DEGs were found in the liver among 3 tissues. However, different patterns of DEGs were identified as the production stage was changed. The liver tissue showed the greatest change in MP vs. EP, whereas the jejunal tissue showed the greatest change in LP vs. MP. However, the uterus tissue showed change at the lesser extent than other tissues, but the greatest change occurred in the uterus tissue between MP vs. EP. Moreover, the result of DEGs consistently demonstrated that the most significant changes were found in the liver, whereas the least change were observed in the uterus throughout all production stages. These findings suggest that gene expression alterations may differ by

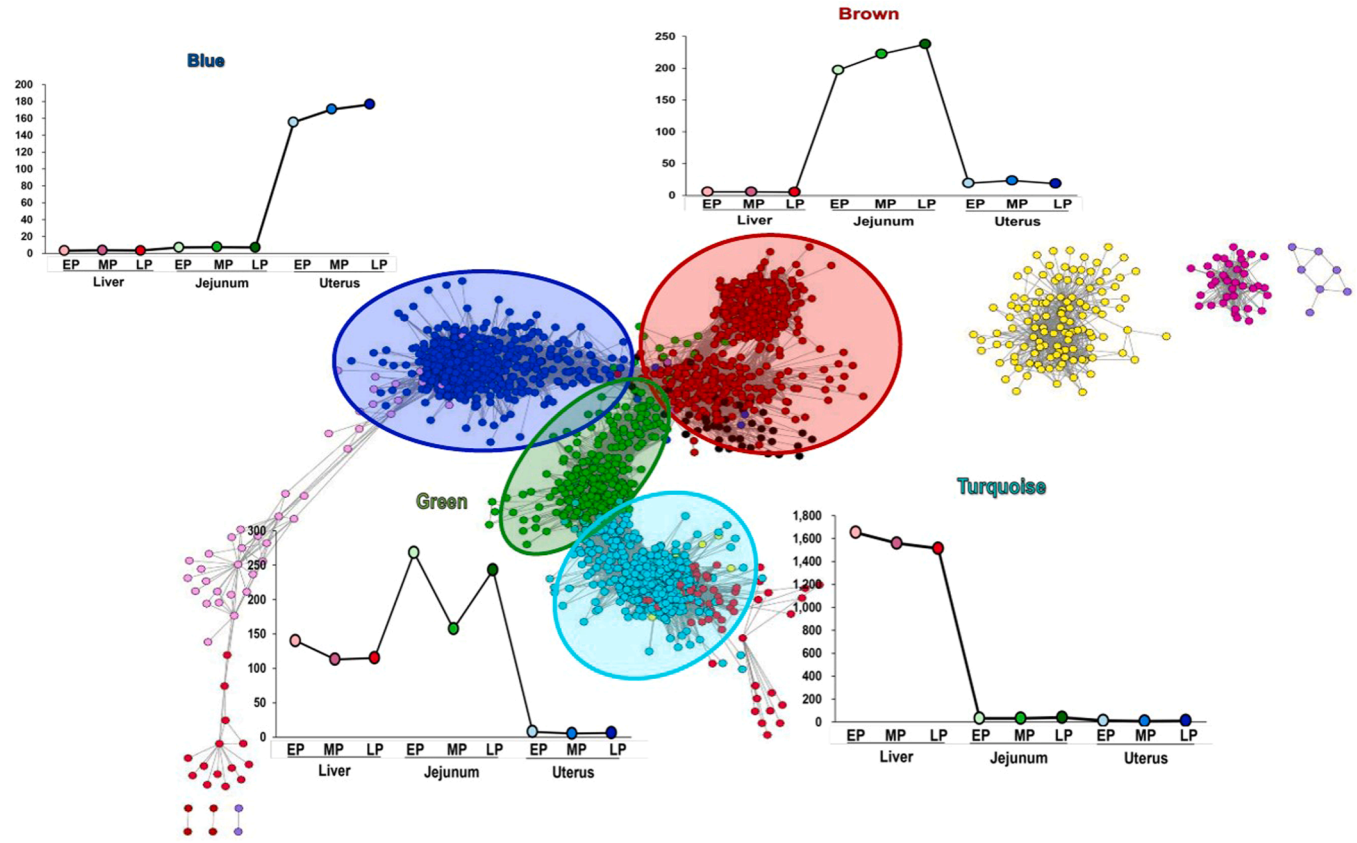

Fig. 6. Weighted gene co-expression network analysis focusing on the important modules (Blue, Brown, Green, and Turquoise). The x and y axes of the graph show according to the different production stage and tissue group, and trimmed mean of M-value (TMM), respectively. The genes in the blue modules are specific expressed in the uterus of laying hens. The genes in the brown and green modules are specific expressed in the jejunum of laying hens. The genes in the turquoise modules are specific expressed in the liver of laying hens.

tissues as the production stage in laying hens progresses.

Among 13 up-regulated genes in MP vs. EP stage for the intersection of 3 tissues, fatty acid elongase 7 (***ELOVL7***) was identified. The *ELOVL7* gene is associated with the synthesis of long-chain saturated fatty acid (**LCFA**) and also the first-rate limiting enzyme in carbon chain elongations of LCFA, which play an important role in the synthesis of lipid complexes (Wang et al., 2022). A previous study reported that aged hens have a high incidence of fatty liver, which accumulated higher contents of triglyceride than young hens (Gu et al., 2021b). According to Liu et al. (2019), the expression of *ELOVL7* was increased in the chicken with high triglyceride contents, indicating that up-regulation of this gene may elevate the synthesis and deposition of triglycerides. In this study, *ELOVL7* was up-regulated commonly in all 3 tissues during MP stage compared with EP stage, indicating that laying hens at MP stage exhibit more active lipid synthesis than those at EP stage.

Functional analysis was conducted in MP vs. EP stages, indicating that significant GO terms included those associated with cellular response, such as copper ion and zinc ion, as well as GO terms related to oxygen transport and cellular oxidant detoxification in biological process category. There were two DEGs, including metallothionein 3 (***MT3***) and metallothionein 4 (***MT4***) in the cellular zinc ion term. Metallothioneins (**MT**) have a significant function in tightly binding zinc ions and acting as an intracellular zinc reservoir (Baltaci et al., 2018). Zinc, which is a critical trace mineral in laying hens, is integral to eggshell formation in the shell gland (Swiatkiewicz and Koreleski, 2008). It is also a key component of carbonic anhydrase, which is essential for bicarbonate metabolism required for eggshell formation (Li et al., 2019). Moreover, it has been reported that dietary zinc supplementation enhances eggshell thickness in aged laying hens (Tsai et al., 2016). In the present study, *MT3* and *MT4* genes were down-regulated in all tissues at MP stage compared with EP stage. Therefore, it is likely that MP stage may exhibit lower affinity for zinc bindings to MT compared with EP stage. These findings may lead us to hypothesize that one possible reason for lowering eggshell strength with increasing age is the declined ability of MT to bind with zinc in laying hens. However, this hypothesis should be validated in further researches.

In the oxygen transport term, hemoglobin alpha subunit D (***HBAD***) and hemoglobin subunit alpha 1 (***HBA1***) are known to be involved in the recovery of oxidative damage caused by reactive oxygen species (**ROS**; Rifkind et al., 2015). *HBAD* and *HBA1* encode distinct subunits of hemoglobin, which implicates an impairment in DNA repair (Gafter-Gvili et al., 2013). The down-regulation of these genes is associated with a lower capacity for antioxidant defense (Li et al., 2022). Our results also showed that the expression level of *HBAD* and *HBA1* genes was decreased in MP stage compared with EP stage. Therefore, it may be speculated that differential expression of *HBAD* and *HBA1* influences the recovery of oxidative damages, representing that laying hens at MP stage may exhibit a lower antioxidant defense capability than those at EP stage.

In the current study, the calcium voltage-gated channel auxiliary subunit alpha2/delta 1 (***CACNA2D1***) gene was down-regulated in the intersection of the liver, jejunum, and uterus between LP and MP stage. *CACNA2D1* gene is related to the calcium channels that mediate the influx of calcium into the cell (Chang et al., 2015). Calcium ions not only perform various biological functions, such as bone formation and hormone secretion regulation, but also are the most crucial ions in egg production (Park and Sohn., 2018). In addition, calcium ions regulate muscle fiber activity and signaling (Kupittayanant et al., 2009). The pathways controlled by calcium ions are closely associated with muscle contraction and relaxation, indicating that calcium plays an important

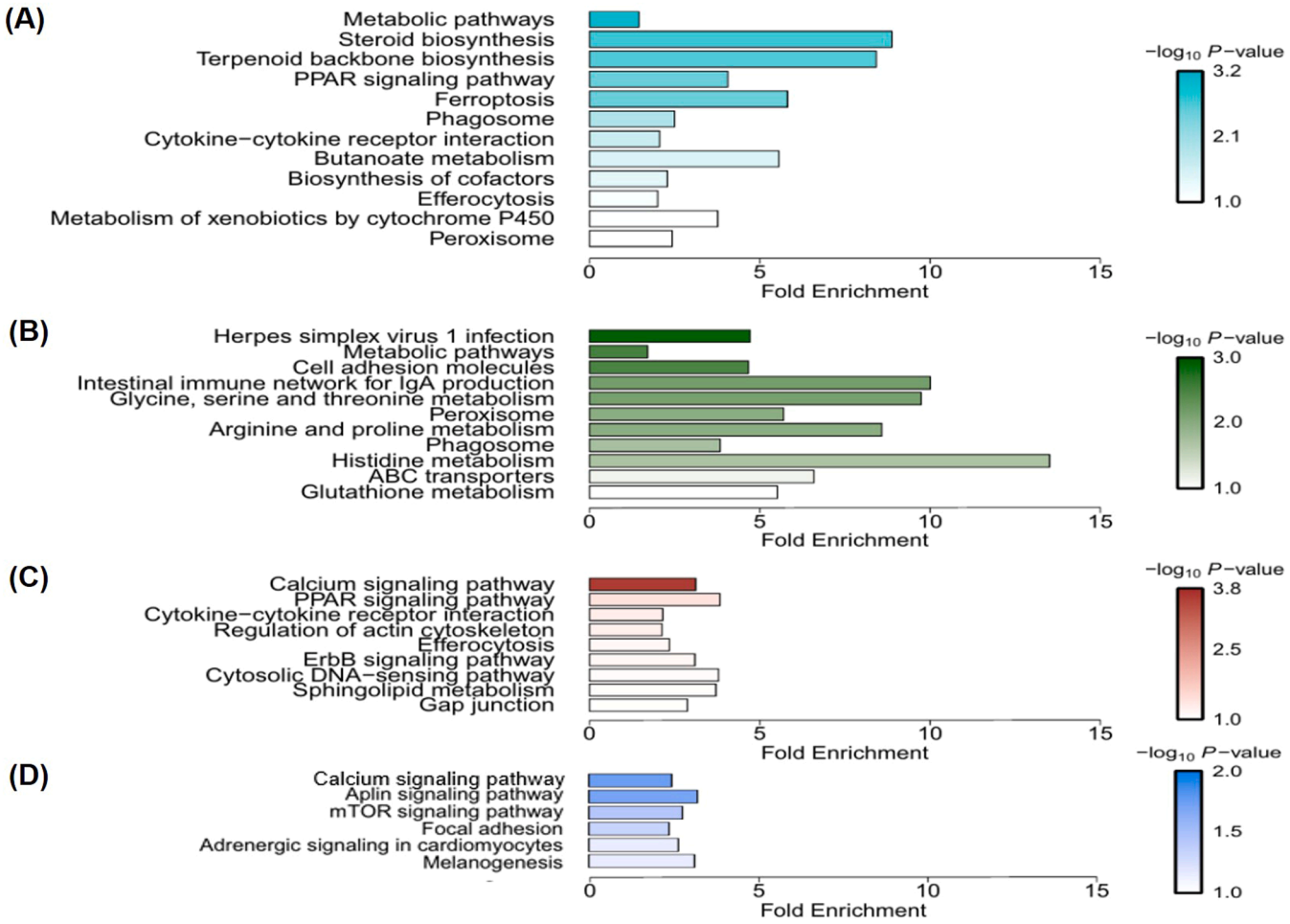

Fig. 7. Enrichment analyses based on the DAVID database according to different production stages of laying hens. KEGG-enriched pathways for each specific network were visualized by bar plot generations. Significantly enriched pathways represented in the plots met the following cut-of criterion: $-\log_{10}$ *P*-value>1.0. (A) Turquoise module. (B) Green module. (C) Brown module. (D) Blue module.

role in regulating uterine muscle contractions (Ledoux et al., 2006; Kupittayanant et al., 2009). However, to our knowledge, no previous studies have revealed the mechanism by which *CACNA2D1* expression affects uterine muscle contraction in laying hens.

In LP vs. EP stage, one DEG (i.e., actin gamma 2, smooth muscle; ***ACTG2***) was identified in the intersection of liver, jejunum, and uterus. *ACTG2*, a member of the actin protein family, plays a crucial role in forming filaments essential for muscle fiber contraction and cellular movement (Li et al., 2024). The uterus of laying hens is sack-shaped, with leaf-like mucosal folds and well-developed muscles (Yin et al., 2019). In this study, the expression of *ACTG2* was decreased in LP vs. EP stage, particularly in the uterus, indicating that the decrease in productive performance of aged laying hens is likely associated with the impairments in uterine smooth muscle contraction. Furthermore, smooth muscle contractions in the uterus plays a crucial role in oviposition (Takahashi et al., 2004). However, research on the molecular physiology of uterine muscle contraction in laying hens is still greatly limited. Therefore, further research is required to validate this hypothesis.

Among 11 DEGs co-expressed in the liver during 3 different production stages, 8 genes exhibited the highest expression in EP stage, whereas 3 genes showed decreased expression levels. ADAM-like decysin 1 (***ADAMDEC1***) belongs to a family of A disintegrin and metalloprotease (**ADAMs**), which is up-regulated in inflammatory conditions in rats with hepatic steatosis (Plaza-Díaz et al., 2017). In this study, *ADAMDEC1* was the most up-regulated in LP stage but was the most down-regulated in EP stage, indicating that aging may lower the ability to cope with inflammation in laying hens. ChaC glutathione-specific gamma-glutamylcyclotransferase 1 (***CHAC1***) is a constituent of the γ-glutamyl cyclotransferase family, participating in the γ-glutamyl cycle. *CHAC1* is capable of degrading glutathione (**GSH**) and is one of several cytosolic enzymes identified for GSH degradation (Kumar et al., 2012; Wanbiao et al., 2024). According to Lian and Tang (2023), *CHAC1* is one of the hub genes related potentially to metabolic dysfunction-associated fatty liver disease (**MAFLD**), indicating that individuals with MAFLD had a lower *CHAC1* expression compared with healthy individuals. In our results, the *CHAC1* genes was most down-regulated in the MP stage. However, it remains unclear why the greatest up-regulation of *CHAC1* in the liver occurs specifically in MP stage.

Most of the DEGs found in the common intersection of different production stages in the jejunum were predominantly down-regulated in LP stage. Among the DEGs in the jejunal intersection, bradykinin receptor B1 (***BDKRB1***) regulates the inflammation (Leschner et al., 2011). In addition, *BDKRB1* belongs to the calcium signaling pathway. According to Luo et al. (2019), the absence of *BDKRB1* led to an increase in bone loss and osteoclast numbers in mice, suggesting that down-regulation of *BDKRB1* may represent disruption of calcium metabolism in bones. Bone-related disorders have been reported to affect egg production and quality in laying hens (Whitehead, 2004). This is because bone damages in laying hens can result in various problems related to calcium metabolism, ultimately affecting eggshell formation

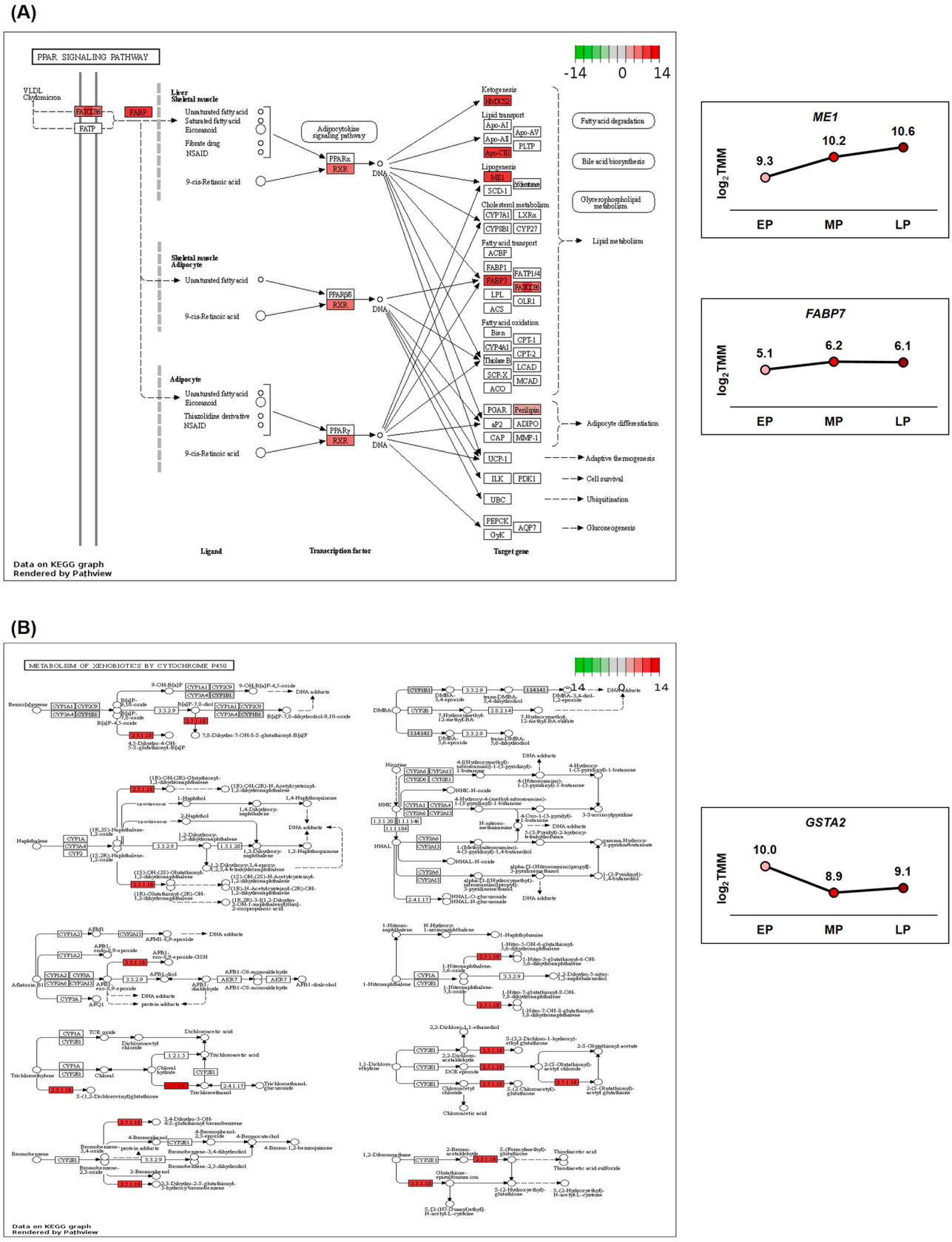

Fig. 8. Gene modulations of the turquoise modules in the liver at the different production stages of laying hens. (A) 'PPAR signaling pathway' (B) 'Metabolism of xenobiotics by cytochrome p450' pathway. The x and y axes of the graph show the different production stage and $\log_2$ trimmed mean of M-value (TMM), respectively. Abbreviation: early-phase (EP, 30-wk-old), mid-phase (MP, 46-wk-old), and late-phase (LP, 60-wk-old) of production stages in laying hens.

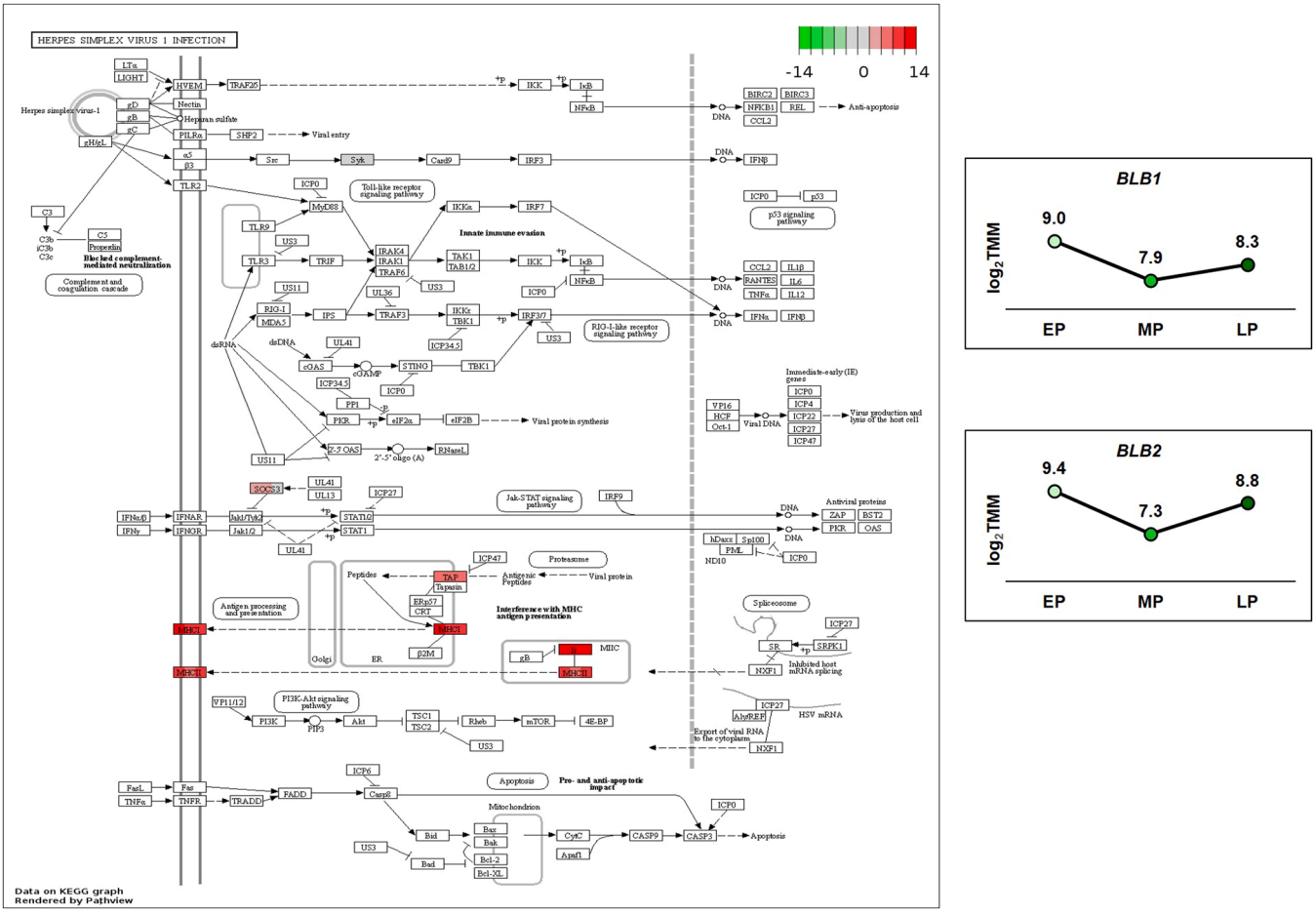

Fig. 9. Gene modulations in 'Herpes simplex virus 1 infection' pathway of the green modules in the jejunum at the different production stages of laying hens. The x and y axes of the graph show the different production stage and $\log_2$ trimmed mean of M-value (TMM), respectively. Abbreviation: early-phase (EP, 30-wk-old), mid-phase (MP, 46-wk-old), and late-phase (LP, 60-wk-old) of production stages in laying hens.

(Whitehead, 2004). In the current study, *BDKRB1* was the most down-regulated in LP stage, indicating that aged laying hens experience a decline in bone-related calcium metabolism. This finding is consistent with the previous observation that bone disorders increase with age in laying hens (Yamada et al., 2021).

In particular, all 21 intersection DEGs in the uterus showed the least expression levels in LP stage. These DEGs are linked to pathways involved in muscle contraction, such as actin and myosin. Pro-opiomelanocortin (***POMC***) is responsible for regulating energy balance and reproduction (Hill et al., 2008). *POMC* plays a role in numerous biological pathways, such as stimulating the release of stress hormone and eggshell-related hormones (Liu et al., 2023). Previous uterine transcriptomic analysis regarding eggshell formation in laying hens demonstrated that decreased expression levels of *POMC* was observed when a weak eggshell was formed in the uterine tissue (Khan et al., 2019). The present study also indicated that *POMC* expression in the uterus was down-regulated in LP stage compared with the other stages. Therefore, it may be speculated that the weak eggshell formation in the uterus during the LP stage is likely associated with a decrease in *POMC* expression.

Approximately half of 21 genes (e.g., *TPM1, LMOD1, SMTN, CNN1, DES, MYL9, TAGLN, ACTG2*, and *ACTA1*) identified at the intersection of the uterus are associated with muscle function, with a notable emphasis on genes specifically related to smooth muscle. Oviposition in laying hens occurs due to the smooth muscle contraction in the uterus, indicating that smooth muscle dysfunction may complicate the oviposition of laying hens (Takahashi et al., 2004). Our results also indicated that the expression of smooth muscle-related genes was mostly down-regulated in LP stage compared with other stages. These findings may lead to a speculation that differential expressions of smooth muscle-related genes influence egg quality, suggesting that aging in laying hens may contribute to a reduced ability to control smooth muscle functions. However, the molecular research regarding uterine muscle functions in laying hens is currently lacking.

Some pathways related to fatty acid metabolism, including steroid biosynthesis and PPAR signaling pathway, were found in the turquoise and brown modules. The PPAR signaling pathway is well-recognized for its significant role in regulating lipid metabolism (Li et al., 2015). Many DEGs identified in the turquoise module of the liver are involved in PPAR signaling pathways, including *FABP3, HMGCS1, FABP7, ME1, APOC3, CD36, PLIN1, and RXRG*. In particular, malic enzyme (***ME1***) is an NADP-dependent enzyme that catalyzes the conversion of l-malate to pyruvate, an important gene involved in lipid synthesis and secretion (Adams and Davis, 2001). In the current study, the expression of *ME1* was increased with age in laying hen. This result may support previous observations indicating a decline in liver health with increasing lipid accumulation by aging in laying hens (Han et al., 2023). According to Zhang et al. (2018), the expression of *ME1* was higher in chickens with fatty liver as compared to those without fatty liver. In addition, fatty acid binding protein 7 (***FABP7***), a critical gene in fatty acid metabolism, also exhibited a similar up-regulation pattern in laying hens. Similarly, several DEGs identified in the brown module of the jejunum are involved in PPAR signaling pathways, including *FABP2, FABP5, MMP1, FABP6*, and *PPARγ*. Most DEGs in the PPAR signaling pathway of the brown

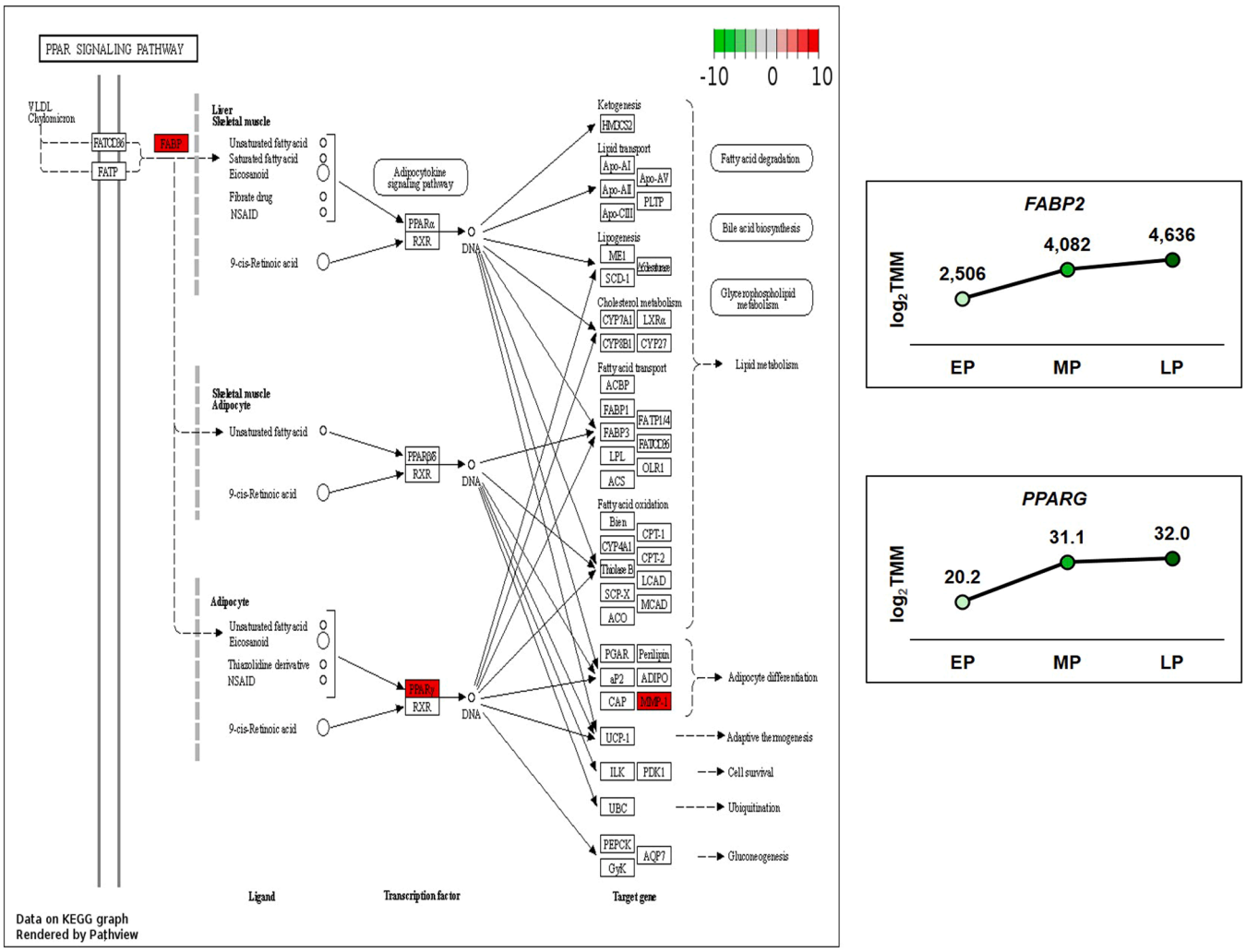

Fig. 10. Gene modulations in 'PPAR signaling pathway' of the brown modules in the jejunum at the different production stages of laying hens. The x and y axes of the graph show the different production stage and $\log_2$ trimmed mean of M-value (TMM), respectively. Abbreviation: early-phase (EP, 30-wk-old), mid-phase (MP, 46-wk-old), and late-phase (LP, 60-wk-old) of production stages in laying hens.

module are associated with fatty acid synthesis. In particular, peroxisome proliferator-activated receptor-gamma (**PPARγ**) plays a significant role in energy expenditure during processes, such as nutrient absorption, digestion, metabolism, and respiratory chain complex activities (Barzegar et al., 2021). Furthermore, PPARγ plays a crucial role in energy partitioning, influencing both fat deposition and egg production in laying hens (Sato et al., 2004). In the present study, the expression of PPARγ was increased with age in laying hens. Therefore, the current multi-tissue transcriptomic profile indicates that lipid synthesis in various tissues is up-regulated with increasing age in laying hens.

Furthermore, the liver is the primary site for xenobiotic detoxification, and cytochrome P450 is a heme-containing enzyme superfamily involved in the metabolism of both exogenous and endogenous xenobiotic substances (Anzenbacher and Anzenbacherová, 2001). In the metabolism of xenobiotics by cytochrome P450 pathway in the turquoise module, glutathione S-transferase alpha 2 (***GSTA2***) contributes to detoxification by attaching glutathione to target electrophilic compounds (Coles and Kadlubar, 2003). *GSTA2* is the predominant glutathione S-transferase expressed in the liver and also exhibits glutathione peroxidase activity, protecting cells against reactive oxygen species and peroxidation by-products (Yang et al., 2018; Zheng et al., 2024). Therefore, the up-regulation of *GSTA2* observed in LP stage may indicate increased liver damage or oxidative stress in laying hens, which is consistent with previous findings that the antioxidant capacity of liver tissues is decreased as laying hens are aged (Gu et al., 2021b).

In herpes simplex virus 1 infection pathway in the green module, major histocompatibility complex class II beta chain BLB1 (***BLB1***), which is involved in immune defense system, is considered a key gene associated with resistance or susceptibility to many poultry diseases (Li et al., 2010). In the current study, *BLB* genes (*BLB1* and *BLB2*) were the most up-regulated in EP stage compared with other stages. It may be speculated that increasing expression of *BLB1* and *BLB2* genes reflects an increase in immune system activation and responses to external stimuli. This observation is likely interpreted as a positive indicator showing that immune defense functions are strengthened in EP stage compared with MP and LP stages. However, it is unclear why immune defense functions in LP stage appears to be higher than in MP stage; however, it can be speculated that increasing oxidaitve and inflammatory damages in LP stage may facilitate immune defense functions as a compensatory mechanism in aging hens.

In green and brown modules related to the jejunum, immune-related pathways were identified, including herpes simplex virus 1 infection, the intestinal immune network for IgA production, and cytokine-cytokine receptor interaction. In the present result, there appears to be a decline in immune functions in MP vs. EP stage; however, it seems to be recovered in LP stage. This result was unexpected because a reduction in immune function is typically observed in aged animals (Feng et al., 2020). However, Schmucker et al. (2021) investigated immune

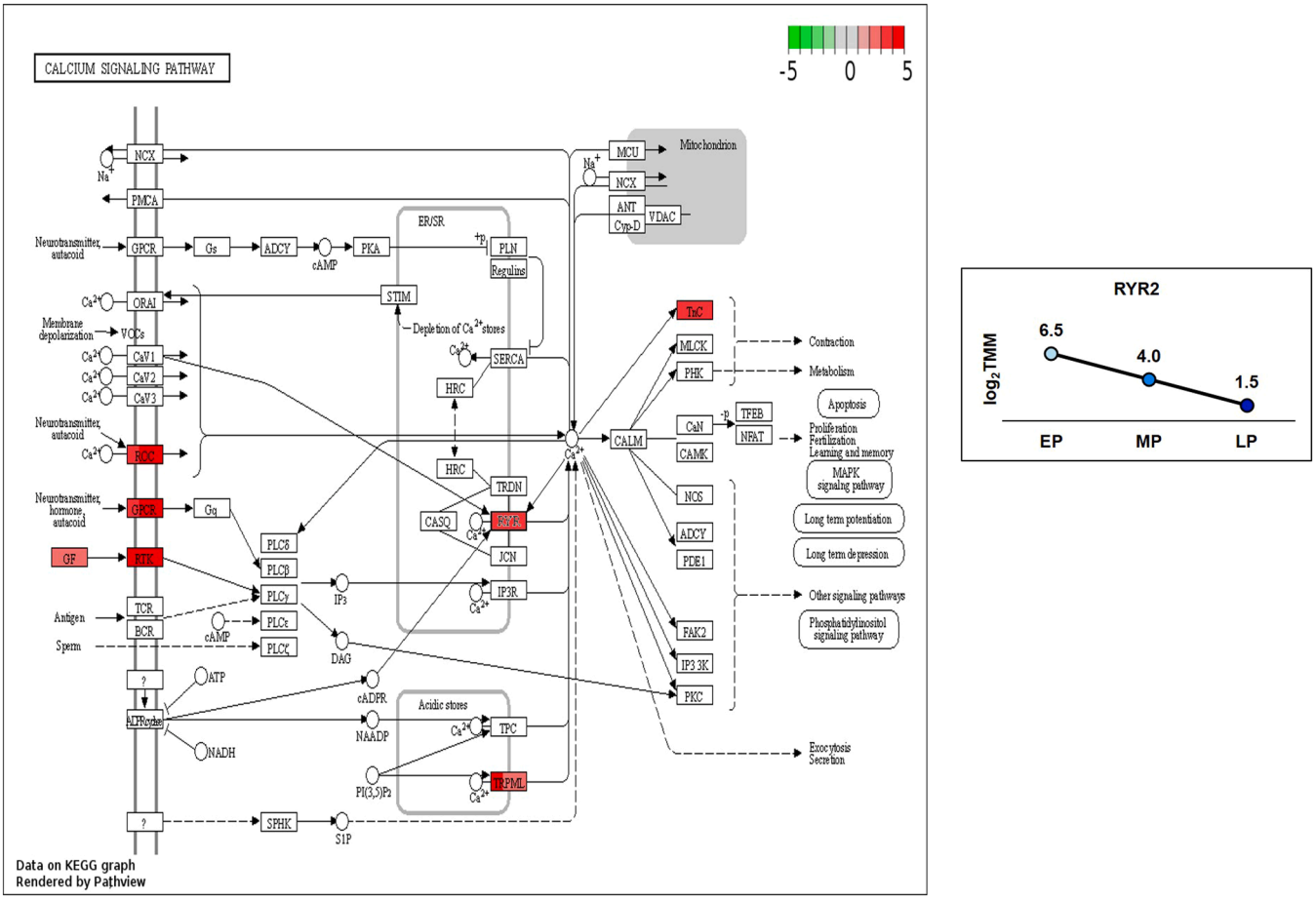

Fig. 11. Gene modulations in 'Calcium signaling pathway' of the blue modules in the uterus at the different production stages of laying hens. The x and y axes of the graph show the different production stage and $\log_2$ trimmed mean of M-value (TMM), respectively. Abbreviation: early-phase (EP, 30-wk-old), mid-phase (MP, 46-wk-old), and late-phase (LP, 60-wk-old) of production stages in laying hens.

parameters in the blood, spleen, and cecal tonsils of laying hens during overall production periods, and reported changes and functions of immune cells for the balance of immune responses with increasing age in laying hens. This observation may suggest that the regulatory mechanisms of the immune system evolve as hens are aged, such that the immune system does not necessarily decline with age. To our knowledge, however, there are no data pertaining to measure the immune response in the jejunum of laying hens as affected by age; therefore, it is difficult to find the clear reason for the current observation.

In the blue module associated with the uterus, most DEGs in the calcium signaling pathway were down-regulated with increasing age in laying hens. Ryanodine receptor 2 (*RYR2*) acts as a component of calcium channels that provide Ca^{2+} for excitation-contraction coupling in cardiac muscle (Wang et al., 2015). According to Ma et al. (2023), the up-regulation of *RYR2* was beneficial to increase calcium ion concentrations in the uterus of laying hens. Therefore, it may be speculated that calcium signaling in the uterus is decreased with age, which may contribute to poor egg quality in aged laying hens.

Conclusion

The present study conducted a multi-tissue transcriptomic analysis with the liver, jejunum, and uterus across different production stages of laying hens. Several genes related to lipid synthesis were up-regulated with increasing age in laying hens. Moreover, various genes associated with age-related alterations regarding mineral utilization, antioxidant system, hormonal response, immune system, calcium signaling, and muscle contraction were also identified as laying hens are aged. These findings provide a potential clue for understanding the molecular mechanism in the liver, jejunum, and uterus across different production stages of laying hens, and therefore, serve as valuable reference data for future research to provide new insights into integrated functions of multiple tissues with increasing age in laying hens.

Declaration of competing interest

The authors declare no conflict of interest for the data presented in this experiment.

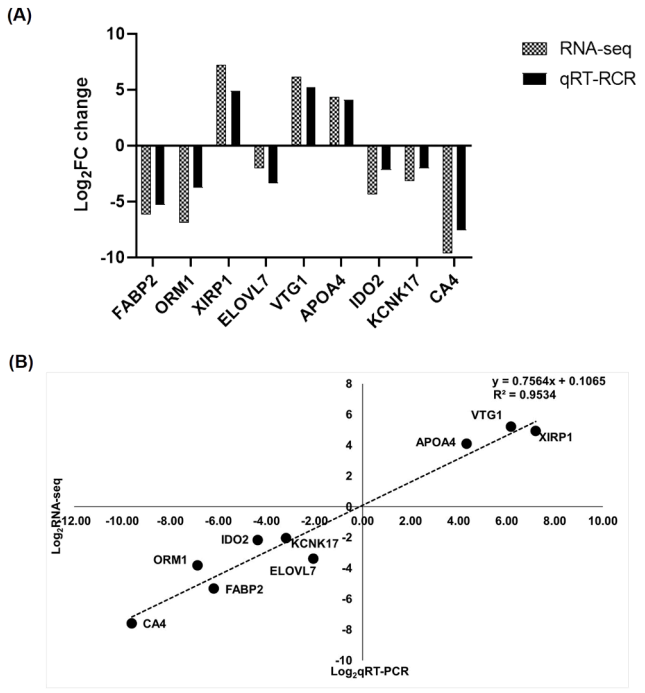

Fig. 12. Illustrating of quantitative reverse-transcription polymerase chain reaction (qRT-PCR) validation for selected differentially expressed genes. The selected genes were placed in x and y axes represents $\log_2$ (fold change) from qRT-PCR and RNA-sequencing. (A) comparison of the mRNA expression levels. (B) linear regression between qRT-PCR and RNA-sequencing.

Acknowledgments

This research was carried out with the support of the Cooperative Research Program for Agriculture Science and Technology Development (Project No. PJ01256701), Rural Development Administration, Republic of Korea. We also thank the BT research facility center, Chung-Ang University.

Supplementary materials

Supplementary material associated with this article can be found, in the online version, at doi:10.1016/j.psj.2025.105329.

References

Adams, K.A., Davis, A.J., 2001. Dietary protein concentration regulates the mRNA expression of chicken hepatic malic enzyme. J. Nutr. 131, 2269–2274.
Andrews S. 2010. FastQC: a quality control tool for high throughput sequence data. http://www.bioinformatics.babraham.ac.uk/projects/fastqc.
Anzenbacher, P., Anzenbacherová, E., 2001. Cytochromes P450 and metabolism of xenobiotics. Cell. Mol. Life Sci. 58, 737–747.
Baltaci, A.K., Yuce, K., Mogulkoc, R., 2018. Zinc metabolism and metallothioneins. Biol. Trace Elem. Res. 183, 22–31.
Barzegar, S., Swick, R.A., Kheravii, S.K., Choct, M., Wu, S.B., 2021. Peroxisome proliferator-activated receptor gamma upregulation and dietary fat levels in laying hens. Poult. Sci. 100, 101049.
Bolger, A.M., Lohse, M., Usadel, B., 2014. Trimmomatic: a flexible trimmer for Illumina sequence data. Bioinformatics 30, 2114–2120.
Boling, S.D., Douglas, M.W., Johnson, M.L., Wang, X., Parsons, C.M., Koelkebeck, K.W., Zimmerman, R.A., 2000. The effects of dietary available phosphorus levels and phytase on performance of young and older laying hens. Poult. Sci. 79, 224–230.
Chang, K.W., Huang, N.A., Liu, I..H., Wang, Y.H., Wu, P., Tseng, Y.T., Hughes, M.W., Jiang, T.X., Tsai, C.Y, Chen, M.H., Oyang, Y.J., Lin, E.C., Chuong, C.M., Lin, S.P., 2015. Emergence of differentially regulated pathways associated with the development of regional specificity in chicken skin. BMC Genom. 16, 22.
Chen, F., Zhang, H., Du, E., Jin, F., Zheng, C., Fan, Q., Zhao, N., Guo, W., Zhang, W., Huang, S., Wei, J., 2021. Effects of magnolol on egg production, egg quality, antioxidant capacity, and intestinal health of laying hens in the late phase of the laying cycle. Poult. Sci. 100, 835–843.
Coles, B.F., Kadlubar, F.F., 2003. Detoxification of electrophilic compounds by glutathione S-transferase catalysis: determinants of individual response to chemical carcinogens and chemotherapeutic drugs? Biofactors 17, 115–130.
de Juan, A.F., Scappaticcio, R., Aguirre, L., Fondevila, G., García, J., Cámara, L., Mateos, G.G., 2023. Influence of the calcium and nutrient content of the prelay diet on egg production, egg quality, and tibiae mineralization of brown egg-laying hens from 16 to 63 wk of age. Poult. Sci. 102, 102491.
Dennis, G., Sherman, B.T., Hosack, D.A., Yang, J., Gao, W., Lane, H.C., Lempicki, R.A., 2003. DAVID: database for annotation, visualization, and integrated discovery. Genome Biol. 4, R60.
El-Sabrout, K., Aggag, S., Mishra, B., 2022. Advanced practical strategies to enhance table egg production. Scientifica 2022, 1393392.
Feng, J., Zhang, H., Wu, S., Qi, G., Wang, J., 2020. Uterine transcriptome analysis reveals mRNA expression changes associated with the ultrastructure differences of eggshell in young and aged laying hens. BMC Genom. 21, 770.
Gafter-Gvili, A., Zingerman, B., Rozen-Zvi, B., Ori, Y., Green, H., Lubin, I., Malachi, T., Gafter, U., Herman-Edelstein, M., 2013. Oxidative stress-induced DNA damage and repair in human peripheral blood mononuclear cells: protective role of hemoglobin. PLoS One 8, e68341.
Galea F. 2011. Nutrition and food management and their influence on egg quality. XLVIII Scientific Symposium of Poultry, Santiago de Compostela, Spain, 5-7 October.
Gu, Y.F., Chen, Y.P., Jin, R., Wang, C., Wen, C., Zhou, Y.M., 2021a. A comparison of intestinal integrity, digestive function, and egg quality in laying hens with different ages. Poult. Sci. 100, 100949.
Gu, Y.F., Chen, Y.P., Jin, R., Wang, C., Wen, C., Zhou, Y.M., 2021b. Age-related changes in liver metabolism and antioxidant capacity of laying hens. Poult. Sci. 100, 101478.
Guo, W., Xu, L., Guo, X., Wang, W., Hao, Q., Wang, S., Zhu, B., 2022. The impacts of fermented feed on laying performance, egg quality, immune function, intestinal morphology and microbiota of laying hens in the late laying cycle. Animal 16, 100676.
Han, G.P., Kim, J.M., Kang, H.K., Kil, D.Y., 2021. Transcriptomic analysis of the liver in aged laying hens with different intensity of brown eggshell color. Anim. Biosci. 34, 811–823.
Han, G.P., Kim, J.H., Kim, J.M., Kil, D.Y., 2023. Transcriptomic analysis of the liver in aged laying hens with different eggshell strength. Poult. Sci. 102, 102217.
Hao, E.Y., Wang, D.H., Chen, Y.F., Zhou, R.Y., Chen, H., Huang, R.L., 2021. The relationship between the mTOR signaling pathway and ovarian aging in peak-phase and late-phase laying hens. Poult. Sci. 100, 334–347.
Hill, J.W., Williams, K.W., Ye, C., Luo, J., Balthasar, N., Coppari, R., Cowley, M.A., Cantley, L.C., Lowell, B.B., Elmquist, J.K., 2008. Acute effects of leptin require PI3K signaling in hypothalamic proopiomelanocortin neurons in mice. J. Clin. Invest. 118, 1796–1805.
Hy-Line Brown International. 2016. Hy-line Brown commercial layer management guide. Hy-Line Int. West Des Moines, IA.
Kaspers B. 2016. An egg a day: the physiology of egg formation. Lohmann Inf. 50:12-17.
Khan, S., Wu, S.B., Roberts, J., 2019. RNA-sequencing analysis of shell gland shows differences in gene expression profile at two time-points of eggshell formation in laying chickens. BMC Genom. 20, 89.
Kim, C.H., Song, J.H., Lee, J.C., Lee, K.W., 2014. Age-related changes in egg quality of Hy-Line brown hens. Int. J. Poult. Sci. 13, 510–514.
Kim, D., Langmead, B., Salzberg, S.L., 2015. HISAT: a fast spliced aligner with low memory requirements. Nat. Methods 12, 357–360.
Kim, D.Y., Han, G.P., Lim, C., Kim, J.M., Kil, D.Y., 2023. Effect of dietary betaine supplementation on the liver transcriptome profile in broiler chickens under heat stress conditions. Anim. Biosci. 36, 1632–1646.
Kumar, A., Tikoo, S., Maity, S., Sengupta, S., Sengupta, S., Kaur, A., Bachhawat, A.K., 2012. Mammalian proapoptotic factor ChaC1 and its homologues function as γ-glutamyl cyclotransferases acting specifically on glutathione. EMBo Rep. 13, 1095–1101.
Kupittayanant, S., Kupittayanant, P., Suwannachat, C., 2009. Mechanisms of uterine contractility in laying hens. Anim. Reprod. Sci. 115, 215–224.
Langfelder, P., Horvath, S., 2008. WGCNA: an R package for weighted correlation network analysis. BMC Bioinform. 9, 559.
Ledoux, J., Werner, M.E., Brayden, J.E., Nelson, M.T., 2006. Calcium-activated potassium channels and the regulation of vascular tone. Physiology 21, 69–79.
Leschner, J., Ring, L., Feierler, J., Dinkel, K., Jochum, M., Faussner, A., 2011. Fever-like temperature modification differentially affects *in vitro* signaling of bradykinin B_1 and B_2 receptors. Biol. Chem. 392, 1021–1029.
Li, C., Wang, Y., Sun, X., Yang, J., Ren, Y., Jia, J., Yang, G., Liao, M., Jin, J., Shi, X., 2024. Identification of different myofiber types in pigs muscles and construction of regulatory networks. BMC Genom. 25, 400.
Li, H., Wang, T., Xu, C., Wang, D., Ren, J., Li, Y., Tian, Y., Wang, Y., Jiao, Y., Kang, X., Liu, X., 2015. Transcriptome profile of liver at different physiological stages reveals potential mode for lipid metabolism in laying hens. BMC Genom. 16, 763.
Li, H., Fang, K., Peng, H., He, L., Wang, Y., 2022. The relationship between glycosylated hemoglobin level and red blood cell storage lesion in blood donors. Transfusion 62, 663–674.
Li, J., Jia, Y., Lin, A., Hanna, M., Chelico, L., Xiao, W., Moore, S.A., 2019. Structure of Ddi2, a highly inducible detoxifying metalloenzyme from *Saccharomyces cerevisiae*. J. Biol. Chem. 294, 10674–10685.
Li, X.X., Han, L.X., Han, J.L., 2010. No specific primer can independently amplify the complete exon 2 of chicken BLB1 or BLB2 genes. Int. J. Poult. Sci. 9, 192–197.
Lian, X., Tang, X., 2023. Use of a ferroptosis-related gene signature to construct diagnostic and prognostic models for assessing immune infiltration in metabolic dysfunction-associated fatty liver disease. Front. Cell Dev. Biol. 11, 1199846.

Liao, Y., Smyth, G.K., Shi, W., 2014. Featurecounts: an efficient general purpose program for assigning sequence reads to genomic features. Bioinformatics 30, 923–930.
Liu, L., Liu, X., Cui, H., Liu, R., Zhao, G., Wen, J., 2019. Transcriptional insights into key genes and pathways controlling muscle lipid metabolism in broiler chickens. BMC Genom. 20, 863.
Liu, Z., Cao, Y., Ai, Y., Lin, G., Yin, X., Wang, L., Wang, M., Zhang, B., Wu, K., Guo, Y., Han, H., 2023. Effects of selenium yeast on egg quality, plasma antioxidants, selenium deposition and eggshell formation in aged laying hens. Animals 13, 902.
Luo, J., Sun, P., Siwko, S., Liu, M., Xiao, J., 2019. The role of GPCRs in bone diseases and dysfunctions. Bone Res. 7, 19.
Ma, W., Lu, Y., Wang, C., 2023. Production performance, egg quality, and uterine gene expression for layers as affected by N-carbamylglutamate supplementation. Front. Vet. Sci. 10, 1110801.
Malila, Y., Uengwetwanit, T., Sanpinit, P., Songyou, W., Srimarut, Y., Knhareang, S., 2024. Thermal impacts on transcriptome of *pectoralis major* muscle collected from commercial broilers, Thai native chickens and its crossbreeds. Anim. Biosci. 37, 61–73.
Mishra, B., Sah, N., Wasti, S., 2019. Genetic and hormonal regulation of egg formation in the oviduct of laying hens. Poultry-An Advanced Learning. IntechOpen, London, UK.
Omotoso, A.O., Reyer, H., Oster, M., Ponsuksili, S., Trakooljul, N., Muráni, E., Sommerfeld, V., Rodehutscord, M., Wimmers, K., 2021. Jejunal transcriptomic profiling of two layer strains throughout the entire production period. Sci. Rep. 11, 20086.
Park, J.A., Sohn, S.H., 2018. The influence of hen aging on eggshell ultrastructure and shell mineral components. Korean J. Food Sci. Anim. Resour. 38, 1080–1091.
Plaza-Díaz, J., Robles-Sánchez, C., Abadía-Molina, F., Morón-Calvente, V., Sáez-Lara, M. J., Ruiz-Bravo, A., Jiménez-Valera, M., Gil, Á., Gómez-Llorente, C., Fontana, L., 2017. *Adamdec1, Ednrb* and *Ptgs1/Cox1,* inflammation genes upregulated in the intestinal mucosa of obese rats, are downregulated by three probiotic strains. Sci. Rep. 7, 1939.
Rifkind, J.M., Mohanty, J.G., Nagababu, E., 2015. The pathophysiology of extracellular hemoglobin associated with enhanced oxidative reactions. Front. Physiol. 5, 500.
Robinson, M.D., Oshlack, A., 2010. A scaling normalization method for differential expression analysis of RNA-seq data. Genome Biol. 11, R25.
Robinson, M.D., McCarthy, D.J., Smyth, G.K., 2010. edgeR: a bioconductor package for differential expression analysis of digital gene expression data. Bioinformatics 26, 139–140.
Sato, K., Fukao, K., Seki, Y., Akiba, Y., 2004. Expression of the chicken peroxisome proliferator-activated receptor-γ gene is influenced by aging, nutrition, and agonist administration. Poult. Sci. 83, 1342–1347.
Schmucker, S., Hofmann, T., Sommerfeld, V., Huber, K., Rodehutscord, M., Stefanski, V., 2021. Immune parameters in two different laying hen strains during five production periods. Poult. Sci. 100, 101408.
Skřivan, M., Marounek, M., Bubancová, I., Podsedníček, M., 2010. Influence of limestone particle size on performance and egg quality in laying hens aged 24–36 weeks and 56–68 weeks. Anim. Feed Sci. Technol. 158, 110–114.
Smyth, G.K., 2005. Limma: linear models for microarray data. Pages 397-420 in. In: Gentleman, R., Cary, V.J., Huber, W., Irizarry, R.A., Dudoit, S. (Eds.), Bioinformatics and Computational Biology Solutions Using R and Bioconductor. Springer, New york, NY. ed.
Swiatkiewicz, S., Koreleski, J., 2008. The effect of zinc and manganese source in the diet for laying hens on eggshell and bones quality. Vet. Med. 53, 555–563.
Takahashi, T., Ogawa, H., Inaba, R., Kawashima, M., 2004. Changes in prostaglandin F concentration in the uterus (shell gland) of the hen oviduct in relation to oviposition and estrogen. Poult. Sci. 83, 1745–1749.
Tsai, Y.H., Mao, S.Y., Li, M.Z., Huang, J.T., Lien, T.F., 2016. Effects of nanosize zinc oxide on zinc retention, eggshell quality, immune response and serum parameters of aged laying hens. Anim. Feed Sci. Technol. 213, 99–107.
Wanbiao, Z., Jing, M., Shi, Z., Tengxiang, C., Xueke, Z., Haiyang, L., 2024. MIA3 promotes the degradation of GSH (glutathione) by binding to CHAC1, thereby promoting the progression of hepatocellular carcinoma. Mol. Cell. Biochem. 479-2769-2784.
Wang, Q., Wang, W., Wang, G., Rodney, G.G., Wehrens, X.H.T., 2015. Crosstalk between RyR2 oxidation and phosphorylation contributes to cardiac dysfunction in mice with Duchenne muscular dystrophy. J. Mol. Cell. Cardiol. 89, 177–184.
Wang, D., Li, X., Zhang, P., Cao, Y., Zhang, K., Qin, P., Guo, Y., Li, Z., Tian, Y., Kang, X., Liu, X., Li, H., 2022. ELOVL gene family plays a virtual role in response to breeding selection and lipid deposition in different tissues in chicken (Gallus gallus). BMC Genom. 23, 705.
Whitehead, C.C., 2004. Overview of bone biology in the egg-laying hen. Poult. Sci. 83, 193–199.
Yamada, M., Chen, C., Sugiyama, T., Kim, W.K., 2021. Effect of age on bone structure parameters in laying hens. Animals 11, 570.
Yang, S., Wang, L.L., Shi, Z., Ou, X., Wang, W., Chen, X., Liu, G., 2018. Transcriptional profiling of liver tissues in chicken embryo at day 16 and 20 using RNA sequencing reveals differential antioxidant enzyme activity. PLoS One 13, e0192253.
Yin, L., Yu, L., Zhang, L., Ran, J., Li, J., Yang, C., Jiang, X., Du, H., Hu, X., Liu, Y., 2019. Transcriptome analysis reveals differentially expressed genes and pathways for oviduct development and defense in prelaying and laying hens. Am. J. Reprod. Immunol. 82, e13159.
Zhang, Y., Liu, Z., Liu, R., Wang, J., Zheng, M., Li, Q., Cui, H., Zhao, G., Wen, J., 2018. Alteration of hepatic gene expression along with the inherited phenotype of acquired fatty liver in chicken. Genes 9, 199.
Zhang, J., Wang, Y., Zhang, C., Xiong, M., Rajput, S.A., Liu, Y., Qi, D., 2019. The differences of gonadal hormones and uterine transcriptome during shell calcification of hens laying hard or weak-shelled eggs. BMC Genom. 20, 707.
Zheng, Q., Xu, X., Weng, J., Li, M., Li, B., Cao, Y., 2024. The elevated expression of serum glutathione reductase in hepatocellular carcinoma and its role in assessing the therapeutic efficacy and prognosis of transarterial chemoembolization. Free Radic. Biol. Med. 221, 225–234.